The edge reinforced cantilever plate strip

The Edge Reinforced Cantilever Plate Strip

Plaques en console et à bord renforcé

Der randversteifte Kragplattenstreifen

HERBERT REISMANN
Professor, Faculty of Engineering and Applied Sciences, State University of New York, Buffalo, New York, U.S.A.

SHENG-HSIUNG CHENG
Graduate Assistant, Faculty of Engineering and Applied Sciences, State University of New York, Buffalo, New York, U.S.A.

I. Introduction

The cantilever plate is a common structural element, and its stress and deformation characteristics have been examined in a series of previous publications. The earliest treatment appears to be due to McGregor [1] and Holl [2] who considered the edge loaded cantilever plate. McGregor applies the method of Fourier integrals to a cantilever plate strip of unbounded length, while Holl considers a plate of finite length and employs the (approximate) method of finite differences. Jaramillo [3] has treated the case of a cantilever strip of unbounded length under the action of an arbitrarily placed concentrated load. The authors of [1] through [3] employ classical plate theory, which neglects shear deformation. A recent study [4] of the edge loaded cantilever plate within the framework of an improved plate theory indicates that shear deformation effects are limited to the vicinity of the (concentrated) edge load and that other regions of the plate are not affected provided the plate width is large compared to the plate thickness, i.e., say $\frac{a}{h} > 10$.

In actual construction practice, it is customary to reinforce the free edge of the cantilever plate by means of a beam, resulting in a general stiffening of the structure. The present investigation is concerned with the case of a cantilever plate strip of finite width rigidly clamped along one of its edges. A beam is monolithically attached to the opposite, parallel, free edge. The plate is unbounded in the direction of the clamped and free edges. A concentrated load is assumed to act on the reinforcing beam which distributes this load to the plate (see Fig. 1).

Nomenclature

Dimensional quantity	Physical description	F-L-T units
$D = \frac{E h^3}{12(1-\nu^2)}$	plate flexural rigidity	$F-L$
E	Young's modulus	F/L^2
h	plate thickness	L
a	width of plate strip	L
P	transverse concentrated load	F
EI	beam flexural rigidity	$F-L^2$
GJ	beam torsional rigidity	$F-L^2$
$\mathrm{Sinh}\,\alpha = \frac{1}{2}(e^{\alpha}-e^{-\alpha})$	hyperbolic sine function of α	
$\mathrm{Cosh}\,\alpha = \frac{1}{2}(e^{\alpha}+e^{-\alpha})$	hyperbolic cosine function of α	

Dimensionless quantity	To convert to dimensional form, multily by	Physical description
x	a	coordinate along clamped edge
y	a	coordinate along the plate width
z	a	coordinate perpendicular to the xy-plane
w	$\frac{D}{P a^2}$	deflection of plate
q	$\frac{P}{a^2}$	load intensity
M_x	P	bending moment per unit length of section of plate perpendicular to the x axis
M_y	P	bending moment per unit length of section of plate perpendicular to the y axis
M_{xy}	P	twisting moment per unit length of a section of the plate perpendicular to the x axis
Q_x	$\frac{P}{a}$	shear force parallel to z axis per unit length of sections of a plate perpendicular to x axis
Q_y	$\frac{P}{a}$	shear force parallel to z axis per unit length of sections of a plate perpendicular to y axis
$k_1 = \frac{EI}{Da}$	1	stiffness ratio of beam flexural rigidity to the product of plate flexural rigidity and plate width
$k_2 = \frac{GJ}{Da}$	1	stiffness ratio of beam torsional rigidity to the product of plate flexural rigidity and plate width
ν	1	Poisson's ratio

II. Basic Equations

According to classical small deflection plate theory, the transverse deflections of the median surface of the plate are characterized by

$$\frac{\partial^4 w}{\partial x^4} + 2\frac{\partial^4 w}{\partial x^2 \partial y^2} + \frac{\partial^4 w}{\partial y^4} = q, \tag{1}$$

where q is the load intensity. The moment and shear stress resultants are related to the deflections by means of the following equations:

$$M_x = -\left(\frac{\partial^2 w}{\partial x^2} + \nu\frac{\partial^2 w}{\partial y^2}\right), \tag{2}$$

$$M_y = -\left(\frac{\partial^2 w}{\partial y^2} + \nu\frac{\partial^2 w}{\partial x^2}\right), \tag{3}$$

$$M_{xy} = -M_{yx} = -(1-\nu)\frac{\partial^2 w}{\partial x\,\partial y}, \tag{4}$$

$$Q_x = -\frac{\partial}{\partial x}\left(\frac{\partial^2 w}{\partial x^2} + \frac{\partial^2 w}{\partial y^2}\right), \tag{5}$$

$$Q_y = -\frac{\partial}{\partial y}\left(\frac{\partial^2 w}{\partial x^2} + \frac{\partial^2 w}{\partial y^2}\right). \tag{6}$$

The infinite cantilever plate strip with a beam reinforcing the free edge is shown in Fig. 1. We introduce the Cartesian co-ordinate system $0xyz$ such that the xy-plane coincides with the median plane of the plate. The x-axis is chosen to coincide with the clamped edge. The constant load P acts on the beam perpendicular to the xy-plane.

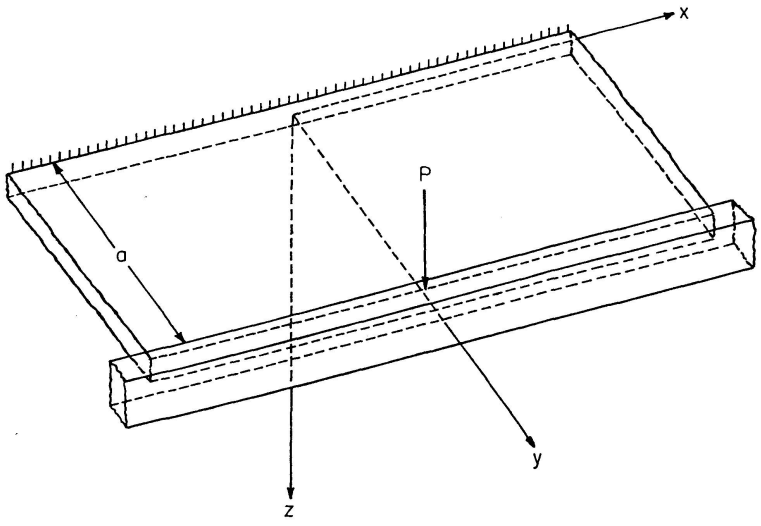

Fig. 1. Plate Strip Geometry.

The governing equation and boundary conditions [5] and [6] are as follows:

$$\frac{\partial^4 w}{\partial x^4}+2\frac{\partial^4 w}{\partial x^2\,\partial y^2}+\frac{\partial^4 w}{\partial y^4}=0, \tag{7}$$

$$w(x,0)=0, \tag{8}$$

$$\frac{\partial}{\partial y}w(x,0)=0, \tag{9}$$

$$k_1\left(\frac{\partial^4 w}{\partial x^4}\right)_{y=1}=\left\{\frac{\partial^3 w}{\partial y^3}+(2-\nu)\frac{\partial^3 w}{\partial x^2\,\partial y}\right\}_{y=1}+\delta(x), \tag{10}$$

$$-k_2\left(\frac{\partial^3 w}{\partial x^2\,\partial y}\right)_{y=1}=\left\{\frac{\partial^2 w}{\partial y^2}+\nu\frac{\partial^2 w}{\partial x^2}\right\}_{y=1}, \tag{11}$$

where Eq. (10) is KIRCHHOFF's condition which is equivalent to the requirements

$$-\left(Q_y-\frac{\partial M_{yx}}{\partial x}\right)_{y=1}=\frac{\partial}{\partial y}\left\{\frac{\partial^2 w}{\partial y^2}+(2-\nu)\frac{\partial^2 w}{\partial x^2}\right\}_{y=1}. \tag{12}$$

III. Solutions for Deflection and Moment

By applying the familiar Fourier Transform [7] with respect to the x-coordinate to the biharmonic Eq. (7), the boundary conditions, Eqs. (8) through (11), and Dirac delta function $\delta(x)$, we have

$$\overline{w}(\alpha,y)=\frac{1}{\sqrt{2\pi}}\int_{-\infty}^{\infty}w(x,y)\,e^{i\alpha x}\,dx \tag{13}$$

with the properties of the transform of the derivative

$$\overline{w}^{(n)}(\alpha,y)=(-i\alpha)^n\,\overline{w}(\alpha,y), \tag{14}$$

where $\overline{w}^{(n)}$ is the nth derivative of $\overline{w}$ with respect to α. The inverse Fourier Transform is

$$w(x,y)=\frac{1}{\sqrt{2\pi}}\int_{-\infty}^{\infty}\overline{w}(\alpha,y)\,e^{-i\alpha x}\,d\alpha. \tag{15}$$

Since

$$\frac{1}{\sqrt{2\pi}}\int_{-\infty}^{\infty}\delta(x)\,e^{i\alpha x}\,dx=\frac{1}{\sqrt{2\pi}} \tag{16}$$

the substitution of Eqs. (13), (14), (16) into Eqs. (7), (8), (9), (10), and (11) leads to

$$\frac{\partial^4}{\partial y^4}\overline{w}(\alpha,y)-2\alpha^2\frac{\partial^2}{\partial y^2}\overline{w}(\alpha,y)+\alpha^4\overline{w}(\alpha,y)=0 \tag{17}$$

with the boundary conditions

$$\overline{w}(\alpha, 0) = 0, \tag{18a}$$

$$\frac{\partial}{\partial y}\overline{w}(\alpha, 0) = 0, \tag{18b}$$

$$k_1 \alpha^4 \overline{w}(\alpha, 1) = \frac{\partial^3}{\partial y^3}\overline{w}(\alpha, 1) - (2-\nu)\alpha^2 \frac{\partial}{\partial y}\overline{w}(\alpha, 1) + \frac{1}{\sqrt{2\pi}}, \tag{18c}$$

$$k_2 \alpha^2 \frac{\partial}{\partial y}\overline{w}(\alpha, 1) = \frac{\partial^2}{\partial y^2}\overline{w}(\alpha, 1) - \nu \alpha^2 \overline{w}(\alpha, 1). \tag{18d}$$

The solution of Eq. (17) is

$$\overline{w}(\alpha, y) = A_1 \operatorname{Sinh} \alpha y + A_2 \alpha y \operatorname{Sinh} \alpha y + A_3 \operatorname{Cosh} \alpha y + A_4 \alpha y \operatorname{Cosh} \alpha y. \tag{19}$$

The coefficients $A_i\,(i = 1, 2, 3, 4)$ are determined from Eq. (18a), (18b), (18c), and (18d) to be

$$A_3 = 0, \tag{20a}$$

$$A_4 = -A_1, \tag{20b}$$

$$A_1 = \frac{1}{\alpha^3 \sqrt{2\pi} f(\alpha)}\{[\alpha k_2 - (1-\nu)\alpha] \operatorname{Sinh} \alpha + (\alpha^2 k_2 - 2) \operatorname{Cosh} \alpha\}, \tag{20c}$$

$$A_2 = \frac{-1}{\alpha^3 \sqrt{2\pi} f(\alpha)}\{[(1+\nu) - \alpha^2 k_2] \operatorname{Sinh} \alpha + (1-\nu)\alpha \operatorname{Cosh} \alpha\}, \tag{20d}$$

where

$$\begin{aligned} f(\alpha) = {} & -2 - \tfrac{1}{2}(1+\nu)^2 + [2k_1 + 2k_2 - (1-\nu)^2 - \tfrac{1}{2} k_1 k_2]\alpha^2 - k_1 k_2 \alpha^4 \\ & - (k_1 - k_2)\alpha \operatorname{Sinh} 2\alpha + \tfrac{1}{2}[-4 + (1+\nu)^2 + k_1 k_2 \alpha^2] \operatorname{Cosh} 2\alpha. \end{aligned} \tag{21}$$

Consequently,

$$\begin{aligned} \overline{w}(\alpha, y) = \frac{1}{\sqrt{2\pi}} \frac{1}{\alpha^3 f(\alpha)} \big[& \{[k_2 - (1-\nu) - (1+\nu) y]\alpha + \alpha^3 k_2 y\} \operatorname{Sinh} \alpha \operatorname{Sinh} \alpha y \\ & + \{[k_2 - (1-\nu) y]\alpha^2 - 2\} \operatorname{Cosh} \alpha \operatorname{Sinh} \alpha y \\ & - [k_2 - (1-\nu)]\alpha^2 y \operatorname{Sinh} \alpha \operatorname{Cosh} \alpha y - (\alpha^3 k_2 - 2\alpha) y \operatorname{Cosh} \alpha \operatorname{Cosh} \alpha y \big]. \end{aligned} \tag{22}$$

Let

$$\begin{aligned} H(\alpha, y) = {} & \{[k_2 - (1-\nu) - (1+\nu) y]\alpha + \alpha^3 k_2 y\} \operatorname{Sinh} \alpha \operatorname{Sinh} \alpha y \\ & + \{[k_2 - (1-\nu) y]\alpha^2 - 2\} \operatorname{Cosh} \alpha \operatorname{Sinh} \alpha y \\ & - [k_2 - (1-\nu)]\alpha^2 y \operatorname{Sinh} \alpha \operatorname{Cosh} \alpha y \\ & - (\alpha^3 k_2 - 2\alpha) y \operatorname{Cosh} \alpha \operatorname{Cosh} \alpha y. \end{aligned} \tag{23}$$

By applying the inverse Fourier Transform, Eq. (15), and with the aid of Eqs. (21), (22), (23), we obtain

$$w(x, y) = \frac{1}{2\pi} \int_{-\infty}^{\infty} \frac{H(\alpha, y)\, e^{-i\alpha x}}{\alpha^3 f(\alpha)} d\alpha. \tag{24}$$

The nondimensionalized moment M_y is determined from Eq. (3). Hence

$$M_y = -\frac{1}{2\pi}\int_{-\infty}^{\infty} \frac{\left(\frac{\partial^2 H}{\partial y^2} - \nu\,\alpha^2 H\right) e^{-i\alpha x}}{\alpha^3 f(\alpha)}\, d\alpha. \tag{25}$$

Let
$$G(\alpha, y) = \frac{1}{\alpha^2}\left(\frac{\partial^2 H}{\partial y^2} - \nu\,\alpha^2 H\right), \tag{26}$$

then

$$\begin{aligned} G(\alpha, y) = &-\{(1+\nu)[k_2-(1-\nu)]\,\alpha + (1-\nu^2)\,\alpha y - (1-\nu)\,\alpha^3 k_2 y\}\,\mathrm{Sinh}\,\alpha\,\mathrm{Sinh}\,\alpha y \\ &-[(1+\nu)(k_2\alpha^2-2)+(1-\nu)^2\alpha^2 y]\,\mathrm{Cosh}\,\alpha\,\mathrm{Sinh}\,\alpha y \\ &+\{2[-(1+\nu)+k_2\alpha^2]-(1-\nu)[k_2-(1-\nu)]\,\alpha^2 y\{\mathrm{Sinh}\,\alpha\,\mathrm{Cosh}\,\alpha y \\ &-[2(1-\nu)\alpha+(1-\nu)(\alpha^3 k_2-2\alpha)y]\,\mathrm{Cosh}\,\alpha\,\mathrm{Cosh}\,\alpha y. \end{aligned} \tag{27}$$

Therefore
$$M_y = -\frac{1}{2\pi}\int_{-\infty}^{\infty} \frac{G(\alpha, y)\, e^{-i\alpha x}}{\alpha f(\alpha)}\, d\alpha. \tag{28}$$

IV. Series Representation of Deflection and Moment

The numerical determination of the deflection and moment as functions of position x and y, the stiffness ratios k_1, k_2 and Poisson's ratio ν, requires evaluation of the improper integrals appearing in Eqs. (24) and (28). In view of the fact that these integrals are not expressible in terms of elementary functions, a numerical integration procedure provides one possible method for their evaluation [1]. However, this approach is exceedingly cumbersome if a complete and sufficiently accurate coverage of the solutions is to be achieved. For this reason, it is advantageous to resort, instead, to contour integration. This method leads to series expansions of the integrals in terms of the residues at the singularities of the corresponding integrands. To this end we observe that the singularities of the integrands in Eqs. (24) and (28) are simple poles and coincide with the zeros of $f(\alpha)$ which, by Eq. (21), are the solutions of

$$\begin{aligned} f(\alpha) = &-2-\tfrac{1}{2}(1+\nu)^2+[2k_1+2k_2-(1-\nu)^2-\tfrac{1}{2}k_1k_2]\,\alpha^2-k_1k_2\alpha^4 \\ &-(k_1-k_2)\,\alpha\,\mathrm{Sinh}\,2\alpha+\tfrac{1}{2}[-4+(1+\nu)^2+k_1k_2\alpha^2]\,\mathrm{Cosh}\,2\alpha, \end{aligned} \tag{21}$$

where $f(\alpha)$ is an even function of α.

Since k_1, k_2 and ν are real and positive, $f(\alpha)$ has no real roots. Moreover, because all coefficients in $f(\alpha)$ are real, the roots of $f(\alpha)$ must occur as complex conjugate pairs.

Considering only the upper half plane, it is readily shown that the roots of Eq. (21) are of the form

$$\alpha_n = \pm\beta_n + i\gamma_n \quad (n = 0, 1, 2, 3, \ldots \infty). \tag{29}$$

Thus in the region under consideration, there is a single purely imaginary root for the specific case $k_1=0$, $k_2=0$, i. e., in the case where the edge beam is absent, the remaining roots occur in complex pairs located symmetrically with respect to the axis of imaginaries. We find that both β_n and γ_n, regardless of the values of ν, k_1, k_2, are monotonically increasing functions of n for $n \geqq 1$

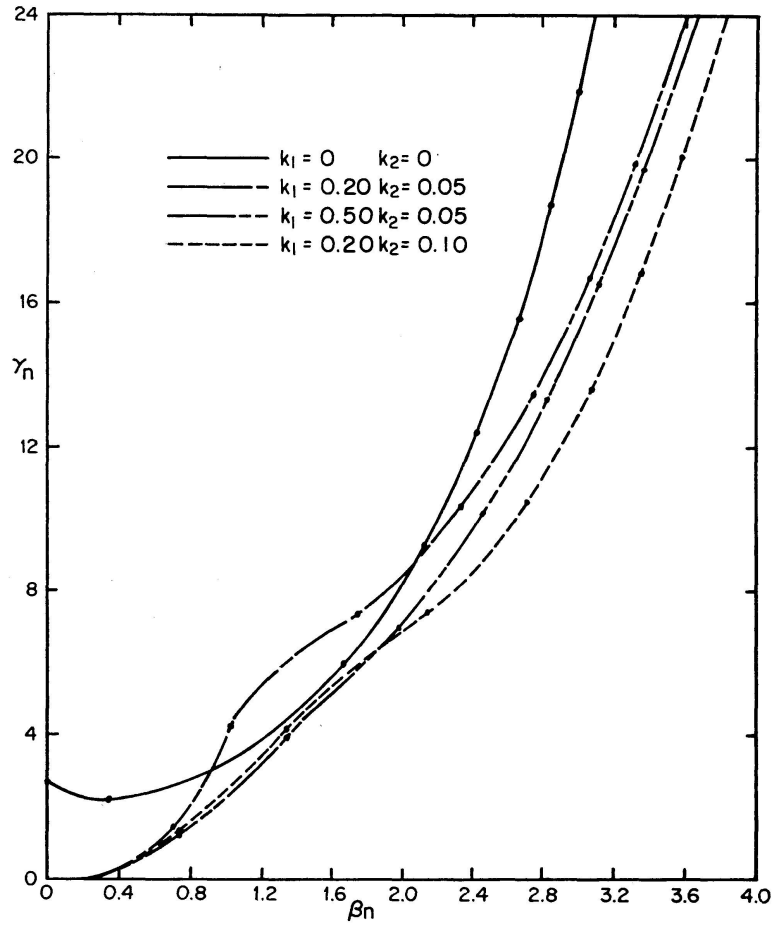

Fig. 2. Location of the Roots α_n of $f(\alpha)=0$.

Table 1. Roots α_n of $f(\alpha) = 0$

n		0	1	2	3	4	5	6	7
$k_1=0$	β_n	0	0.3565	1.6741	2.1312	2.4345	2.6642	2.8498	3.0057
$k_2=0$	γ_n	2.7068	2.0272	5.9638	9.1813	12.3647	15.5341	18.6958	21.8528
$k_1=0.20$	β_n		0.7181	1.0191	1.7462	2.3264	2.7465	3.0666	3.3217
$k_2=0.05$	γ_n		1.4743	4.2396	7.1540	10.2718	13.4398	16.6192	19.8005
$k_1=0.50$	β_n		0.7348	1.3496	1.9759	2.4565	2.8242	3.1153	3.3532
$k_2=0.05$	γ_n		1.2272	3.9520	6.9883	10.1408	13.3246	16.5153	19.7056
$k_1=0.20$	β_n		0.7581	1.3303	2.1532	2.7075	3.0844	3.3607	3.5758
$k_2=0.10$	γ_n		1.4568	4.1722	7.2043	10.4040	13.6182	16.8230	20.0164

and tend to infinity together with n. It is interesting to note that for large values of n, all values of γ_n assymptotically approach $n\pi$.

The distribution of the roots of $f(\alpha)=0$ in the first quandrant of the complex plane is indicated in Fig. 2, which is based on the values of β_n and γ_n for $n=0, 1, 2, \ldots 7$ for $k_1=k_2=0$, and for $n=1, 2, 3, \ldots 7$ for the remaining cases, all of which are given in Table 1. These values are obtained by the combined application of the method of two-dimensional lattices and nets, and the method of false position [9] to the solution of the two real, transcendental equations corresponding to the complex Eq. (21).

By virtue of the Residue Theorem [8], the improper integrals of both deflection, Eq. (24), and moment, Eq. (28), are determined in terms of infinite series as

$$\int_{-\infty}^{\infty} \frac{H(\alpha, y)\, e^{-i\alpha x}}{\alpha^3 f(\alpha)} d\alpha = 2\pi i \sum_{n=0}^{\infty} R_{n1} \tag{30}$$

and

$$\int_{-\infty}^{\infty} \frac{G(\alpha, y)\, e^{-i\alpha x}}{\alpha f(\alpha)} d\alpha = 2\pi i \sum_{n=0}^{\infty} R_{n2}, \tag{31}$$

where $f(\alpha)$, $H(\alpha, y)$, $G(\alpha, y)$ are given by Eqs. (21), (23), (27), respectively. R_{n1} and R_{n2} are the residues at the simple poles α_n of the integrands of both Eq. (30) and Eq. (31), respectively. Therefore, the combination of Eqs. (21), (23), (30) leads to

$$w(x, y) = i \sum_{n=0}^{\infty} \frac{H(\alpha_n, y)\, e^{-i\alpha_n x}}{\alpha_n^3 f'(\alpha_n)} \tag{32}$$

and from Eq. (21), (27), (31), we have

$$M_y(x, y) = i \sum_{n=0}^{\infty} \frac{G(\alpha_n, y)\, e^{-i\alpha_n x}}{\alpha_n f'(\alpha_n)}. \tag{33}$$

Let

$$S_1 = \mathrm{Sinh}(\beta_n), \quad C_1 = \mathrm{Cosh}(\beta_n), \quad s_1 = \mathrm{Sin}(\gamma_n), \quad c_1 = \mathrm{Cos}(\gamma_n),$$
$$S_2 = \mathrm{Sinh}(\beta_n y), \quad C_2 = \mathrm{Cosh}(\beta_n y), \quad s_2 = \mathrm{Sin}(\gamma_n y), \quad c_2 = \mathrm{Cos}(\gamma_n y),$$
$$R_n = \frac{1}{\beta_n^2 + \gamma_n^2}, \qquad \omega_n = \beta_n^2 - \gamma_n^2, \qquad z_n = 2\beta_n\gamma_n,$$
$$U_n = \beta_n^3 - 3\beta_n\gamma_n^2, \qquad V_n = 3\beta_n^2\gamma_n - \gamma_n^3,$$

$$\begin{aligned} E_n = {} & [4k_1 + 4k_2 - 2(1-\nu)^2 - k_1 k_2]\beta_n - 4k_1 k_2 U_n + 2[\omega_n k_1 k_2 - k_1 + k_2 \\ & + (1+\nu)^2 - 4] S_1 C_1 (c_1^2 - s_1^2) - 2 z_n k_1 k_2 s_1 c_1 (C_1^2 + S_1^2) \\ & + (-2k_1 + 2k_2 + k_1 k_2)[\beta_n (C_1^2 + S_1^2)(c_1^2 - s_1^2) - 4\gamma_n S_1 C_1 s_1 c_1], \end{aligned}$$

$$\begin{aligned} F_n = {} & [4k_1 + 4k_2 - 2(1-\nu)^2 - k_1 k_2]\gamma_n - 4k_1 k_2 V_n + 2[\omega_n k_1 k_2 - k_1 + k_2 \\ & + (1+\nu)^2 - 4] s_1 c_1 (C_1^2 + S_1^2) + 2 z_n k_1 k_2 S_1 C_1 (c_1^2 - s_1^2) \\ & + (-2k_1 + 2k_2 + k_1 k_2)[\gamma_n (C_1^2 + S_1^2)(c_1^2 - s_1^2) + 4\beta_n S_1 C_1 s_1 c_1]. \end{aligned}$$

The differentiation of Eq. (21) with respect to α, and the subsequent substitution of α_n for α results in Eq. (34);

$$f'(\alpha_n) = E_n + i F_n. \tag{34}$$

Let
$$f_n = \frac{E_n}{E_n^2 + F_n^2}, \qquad g_n = \frac{F_n}{E_n^2 + F_n^2}. \tag{35}$$

The dimensionless deflection and moment will depend on the parameters k_1, k_2 and Poisson's ratio ν. Let $\nu = 0.3$ and group the values of k_1 and k_2 as follows:

1. The absence of on edge beam, i.e., $k_1 = 0$, $k_2 = 0$. Combine the Eqs. (23), (32), (34) and (35) to obtain

$$\begin{aligned} w(x,y) = \frac{\psi_0}{g_0} - 2\sum_{n=1}^{\infty} e^{\gamma_n x}[f_n(\phi_n \operatorname{Cos}\beta_n x - \psi_n \operatorname{Sin}\beta_n x) \\ - g_n(\psi_n \operatorname{Cos}\beta_n x + \phi_n \operatorname{Sin}\beta_n x)], \end{aligned} \tag{36}$$

where

$$\begin{aligned} \psi_0 = &-\left\{[-k_2 + (1-\nu) + (1+\nu)y]\frac{1}{\gamma_0^2} + k_2 y\right\} \operatorname{Sin}\gamma_0 \operatorname{Sin}\gamma_0 y \\ &+\left\{[k_2 - (1-\nu)y]\frac{1}{\gamma_0} + \frac{2}{\gamma_0^3}\right\} \operatorname{Cos}\gamma_0 \operatorname{Sin}\gamma_0 y \\ &-[k_2 - (1-\nu)]\frac{y}{\gamma_0} \operatorname{Sin}\gamma_0 \operatorname{Cos}\gamma_0 y - \left(k_2 + \frac{2}{\gamma_0^2}\right) y \operatorname{Cos}\gamma_0 \operatorname{Cos}\gamma_0 y, \end{aligned} \tag{37}$$

$$\begin{aligned} g_0 = &[4k_1 + 4k_2 - 2(1-\nu)^2 - k_1 k_2]\gamma_0 + 4k_1 k_2 \gamma_0^3 \\ &+[-\gamma_0^2 k_1 k_2 - k_1 + k_2 + (1+\nu)^2 - 4] \operatorname{Sin} 2\gamma_0 \\ &+[-2k_1 + 2k_2 + k_1 k_2]\gamma_0 \operatorname{Cos} 2\gamma_0, \end{aligned} \tag{38}$$

$$\begin{aligned} \psi_n = &\{[k_2 - (1-\nu) - (1+\nu)y] R_n^2 \omega_n + k_2 y\}(S_1 S_2 c_1 c_2 - C_1 C_2 s_1 s_2) \\ &+[k_2 - (1-\nu) - (1+\nu)y] R_n^2 z_n (S_1 C_2 c_1 s_2 + C_1 S_2 s_1 c_2) \\ &+\{[k_2 - (1-\nu)y] R_n \beta_n - 2R_n^3 U_n\}(C_1 S_2 c_1 c_2 - S_1 C_2 s_1 s_2) \\ &+\{[k_2 - (1-\nu)y] R_n \gamma_n - 2R_n^3 V_n\}(C_1 C_2 c_1 s_2 + S_1 S_2 s_1 c_2) \\ &-[k_2 - (1-\nu)]y R_n[\beta_n (S_1 C_2 c_1 c_2 - C_1 S_2 s_1 s_2) \\ &+\gamma_n (S_1 S_2 c_1 s_2 + C_1 C_2 s_1 c_2) - k_2 y (C_1 C_2 c_1 c_2 - S_1 S_2 s_1 s_2) \\ &+2R_n^2 y[\omega_n (C_1 C_2 c_1 c_2 - S_1 S_2 s_1 s_2) + z_n (C_1 S_2 c_1 s_2 + S_1 C_2 s_1 c_2)], \end{aligned} \tag{39}$$

$$\begin{aligned} \phi_n = &\{[k_2 - (1-\nu) - (1+\nu)y] R_n^2 \omega_n + k_2 y\}(S_1 C_2 c_1 s_2 + C_1 S_2 s_1 c_2) \\ &-\{[k_2 - (1-\nu) - (1+\nu)y] R_n^2 z_n\}(S_1 S_2 c_1 c_2 - C_1 C_2 s_1 s_2) \\ &+\{[k_2 - (1-\nu)y] R_n \beta_n - 2R_n^3 U_n\}(C_1 C_2 c_1 s_2 + S_1 S_2 s_1 c_2) \\ &-\{[k_2 - (1-\nu)y] R_n \gamma_n - 2R_n^3 V_n\}(C_1 S_2 c_1 c_2 - S_1 C_2 s_1 s_2) \\ &-[k_2 - (1-\nu)]y R_n[\beta_n (S_1 S_2 c_1 s_2 + C_1 C_2 s_1 c_2) \\ &-\gamma_n (S_1 C_2 c_1 c_2 - C_1 S_2 s_1 s_2)] - k_2 y (C_1 S_2 c_1 s_2 + S_1 C_2 s_1 c_2) \\ &+2R_n^2 y[\omega_n (C_1 S_2 c_1 s_2 + S_1 C_2 s_1 c_2) - z_n (C_1 C_2 c_1 c_2 - S_1 S_2 s_1 s_2)] \end{aligned} \tag{40}$$

and f_n, g_n are given in Eq. (35).

From Eq. (27), (33), (34) and (35)

$$M_y = \frac{P_0}{g_0} - 2\sum_{n=1}^{\infty} e^{\gamma_n x}\left[f_n\left(Q_n \operatorname{Cos}\beta_n x - P_n \operatorname{Sin}\beta_n x\right) - g_n\left(P_n \operatorname{Cos}\beta_n x + Q_n \operatorname{Sin}\beta_n x\right)\right], \qquad x \leqq 0 \tag{41}$$

where

$$\begin{aligned} P_0 &= \{(1+\nu)[k_2-(1-\nu)]+(1-\nu^2)y+(1-\nu)\gamma_0^2 k_2 y\}\operatorname{Sin}\gamma_0\operatorname{Sin}\gamma_0 y \\ &+\left[(1+\nu)\left(k_2\gamma_0+\frac{2}{\gamma_0}\right)+(1-\nu)^2\gamma_0 y\right]\operatorname{Cos}\gamma_0\operatorname{Sin}\gamma_0 y \\ &-\left\{2\left(\frac{1+\nu}{\gamma_0}+k_2\gamma_0\right)-(1-\nu)[k_2-(1-\nu)]\gamma_0 y\right\}\operatorname{Sin}\gamma_0\operatorname{Cos}\gamma_0 y \\ &-(1-\nu)[2+(\gamma_0^2 k_2-2)y]\operatorname{Cos}\gamma_0\operatorname{Cos}\gamma_0 y, \end{aligned} \tag{42}$$

$$\begin{aligned} P_n &= -\{(1+\nu)[k_2-(1-\nu)]+(1-\nu^2)y-(1-\nu)k_2 y\,\omega_n\}(S_1S_2c_1c_2-C_1C_2s_1s_2) \\ &-(1-\nu)k_2 y z_n(S_1C_2c_1s_2+C_1S_2s_1c_2) \\ &-[(1+\nu)(k_2-2R_n)+(1-\nu)^2 y]\beta_n(C_1S_2c_1c_2-S_1C_2s_1s_2) \\ &+\gamma_n[(1+\nu)(k_2+2R_n)+(1-\nu)^2 y](C_1C_2c_1s_2+S_1S_2s_1c_2) \\ &+\beta_n\{-2R_n(1+\nu)+2k_2-(1-\nu)[k_2-(1-\nu)]y\}(S_1C_2c_1c_2-C_1S_2s_1s_2) \\ &-\gamma_n\{2R_n(1+\nu)+2k_2-(1-\nu)[k_2-(1-\nu)]y\}(S_1S_2c_1s_2+C_1C_2s_1c_2) \\ &-(1-\nu)[2+(k_2\omega_n-2)y](C_1C_2c_1c_2-S_1S_2s_1s_2) \\ &+(1-\nu)k_2 z_n y(C_1S_2c_1s_2+S_1C_2s_1c_2), \end{aligned} \tag{43}$$

$$\begin{aligned} Q_n &= (1-\nu)k_2 y z_n(S_1S_2c_1c_2-C_1C_2s_1s_2)-\{(1+\nu)[k_2-(1-\nu)] \\ &+(1-\nu^2)y-(1-\nu)k_2 y\,\omega_n\}(S_1C_2c_1s_2+C_1S_2s_1c_2) \\ &-\beta_n[(1+\nu)(k_2-2R_n)+(1-\nu)^2 y](C_1C_2c_1s_2+S_1S_2s_1c_2) \\ &-\gamma_n[(1+\nu)(k_2+2R_n)+(1-\nu)^2 y](C_1S_2c_1c_2-S_1C_2s_1s_2) \\ &+\beta_n\{-2R_n(1+\nu)+2k_2-(1-\nu)[k_2-(1-\nu)]y\}(S_1S_2c_1s_2+C_1C_2s_1c_2) \\ &+\gamma_n\{2R_n(1+\nu)+2k_2-(1-\nu)[k_2-(1-\nu)]y\}(S_1C_2c_1c_2-C_1S_2s_1s_2) \\ &-(1-\nu)[2+(k_2\omega_n-2)y](C_1S_2c_1s_2+S_1C_2s_1c_2) \\ &-(1-\nu)k_2 z_n y(C_1C_2c_1c_2-S_1S_2s_1s_2) \end{aligned} \tag{44}$$

where g_0, f_n, g_n, are the same as before.

Table 2. Deflection (w) along $x = 0$

y	$k_1=0$ $k_2=0$	$k_1=0.20$ $k_2=0.05$	$k_1=0.50$ $k_2=0.05$	$k_1=0.20$ $k_2=0.10$
0	0	0	0	0
0.25	0.0134	0.0129	0.0118	0.0129
0.50	0.0500	0.0457	0.0423	0.0463
0.75	0.1003	0.0940	0.0862	0.0949
1.00	0.1677	0.1530	0.1394	0.1568

The results of the calculations of the deflection and moment are given in Tables 2, 3, and 4, and are shown graphically in Figs. 3, 4, and 5.

Table 3. Deflection (w) along Beam Coordinate $y = 1$

x	$k_1=0$ $k_2=0$	$k_1=0.20$ $k_2=0.05$	$k_1=0.50$ $k_2=0.05$	$k_1=0.20$ $k_2=0.10$
0	0.1677	0.1530	0.1394	0.1568
±0.25	0.1494	0.1420	0.1318	0.1449
±0.50	0.1211	0.1200	0.1152	0.1218
±0.75	0.0929	0.0956	0.0953	0.0965
±1.00	0.0685	0.0728	0.0756	0.0730
±1.25	0.0490	0.0535	0.0578	0.0531
±1.50	0.0342	0.0380	0.0427	0.0373
±1.75	0.0234	0.0261	0.0305	0.0252
±2.00	0.0157	0.0174	0.0210	0.0164
±2.25	0.0104	0.0111	0.0139	0.0102
±2.50	0.0068	0.0069	0.0087	0.0060

Table 4. Bending Moment ($-M_y$) along Clamped Edge

x	$k_1=0$ $k_2=0$	$k_1=0.20$ $k_2=0.05$	$k_1=0.50$ $k_2=0.05$	$k_1=0.20$ $k_2=0.10$
0	0.5090	0.4708	0.4295	0.4724
±0.25	0.4740	0.4424	0.4097	0.4448
±0.50	0.3893	0.3785	0.3604	0.3820
±0.75	0.2915	0.2987	0.2961	0.3020
±1.00	0.2053	0.2218	0.2306	0.2240
±1.25	0.1389	0.1571	0.1719	0.1579
±1.50	0.0913	0.1070	0.1233	0.1066
±1.75	0.0587	0.0701	0.0851	0.0690
±2.00	0.0372	0.0442	0.0563	0.0426
±2.25	0.0232	0.0266	0.0354	0.0248
±2.50	0.0143	0.0150	0.0207	0.0133

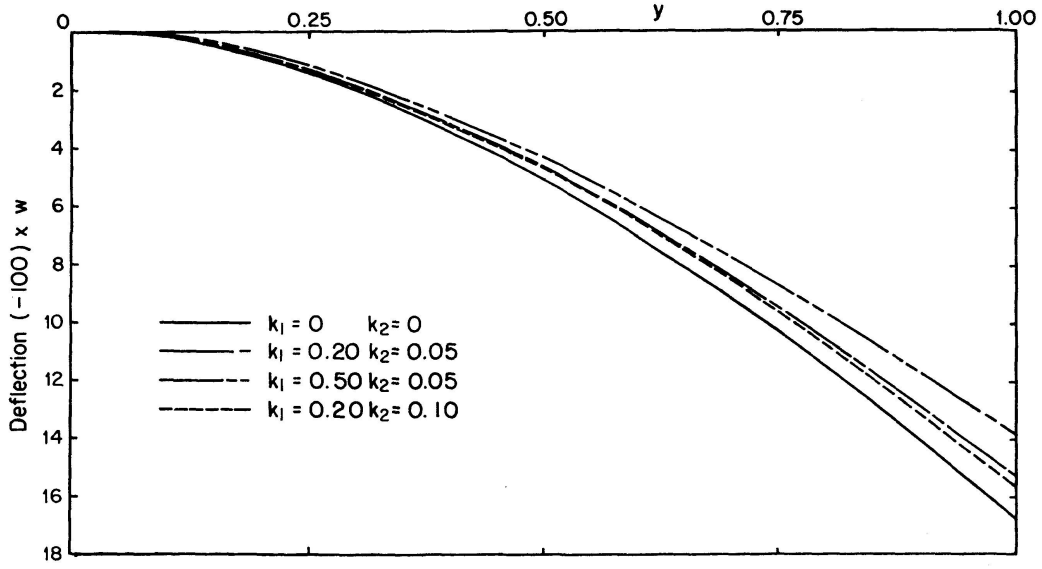

Fig. 3. Profiles of Deflection along $x=0$.

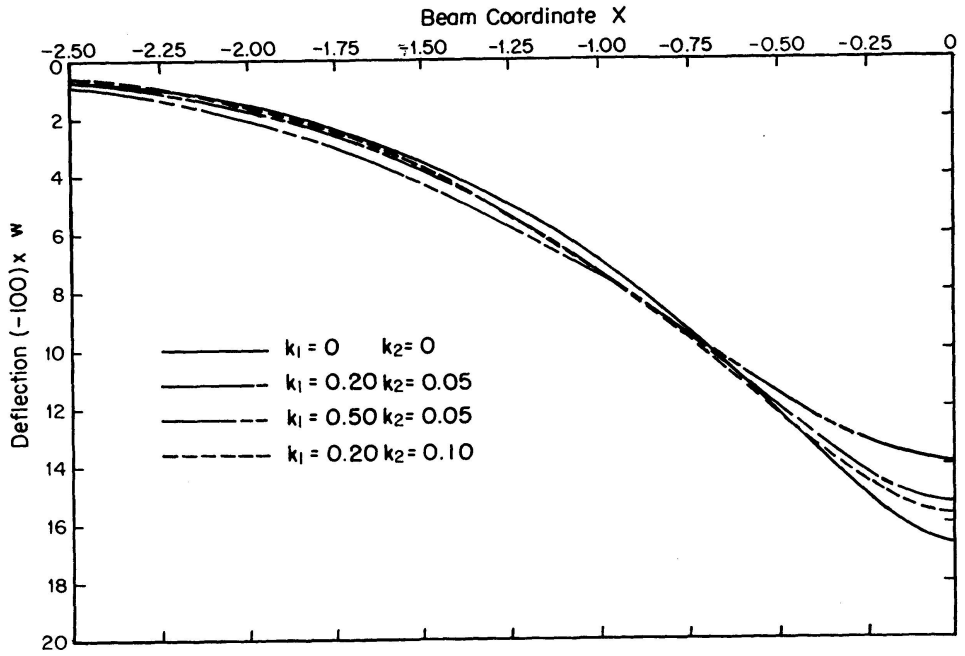

Fig. 4. Profiles of Deflection along Beam. Co-ordinate ($y=1$).

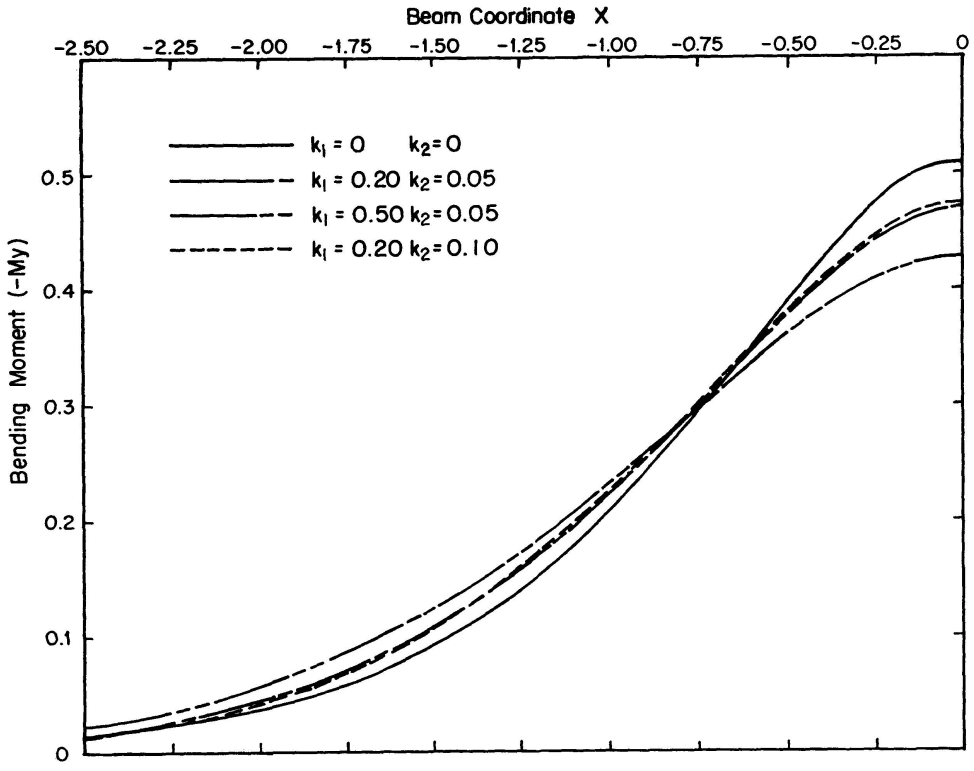

Fig. 5. Bending Moment ($-M_y$) along Clamped Edge.

2. $k_1 \neq 0$, $k_2 \neq 0$.

Use the same argument as in case 1.

$$w(x,y) = -2\sum_{n=1}^{\infty} e^{\gamma_n x}[f_n(\phi_n \operatorname{Cos}\beta_n x - \psi_n \operatorname{Sin}\beta_n x) - g_n(\psi_n \operatorname{Cos}\beta_n x + \phi_n \operatorname{Sin}\beta_n x)], \qquad x \leqq 0 \tag{45}$$

and
$$M_y(x,y) = -2\sum_{n=1}^{\infty} e^{\gamma_n x}(f_n(Q_n \operatorname{Cos}\beta_n x - P_n \operatorname{Sin}\beta_n x) - g_n(P_n \operatorname{Cos}\beta_n x + Q_n \operatorname{Sin}\beta_n x)], \qquad x \leqq 0 \tag{46}$$

where the functions f_n, g_n, φ_n, ψ_n, P_n, and Q_n are defined as in case 1.

These results are also given in Tables 2, 3, and 4, and plotted in Figs. 3, 4, and 5.

The infinite series were truncated after four terms. This yields sufficient accuracy for the deflection and moment in most engineering applications.

3. $k_1 \to \infty$, $k_2 \to \infty$.

This means the beam is rigid. There is no deflection, and the moment M_y is zero along the clamped edge.

V. Discussion of Results and Conclusions

The major results of this investigation are embodied in Figs. 3 through 5. All numerical computations were carried out for Poisson's ratio $\nu = 0.3$. Although no specific cross-sectional shape has been assumed for the stiffening beam, the curves are applicable to the case of a beam of rectangular cross-section with sides h' and b as follows:

$\frac{k_1}{k_2}$	2	4	10
$\frac{h'}{b}$ (approx.)	1.2	2.1	3.55

We note that the limiting case of a beam which is completely limber with respect to flexure and torsion results when $k_1 = k_2 = 0$. The numerical results so obtained are in complete agreement with reference [3], except that data of reference [3] must be divided by π to account for the present non-dimensionalization.

With reference to Figs. 3 through 5, we note that changes of the (non-dimensional) flexural stiffness of the beam k_1 have a more pronounced effect upon deflection and stresses than corresponding changes in its (non-dimensional) torsional stiffness k_2. In the physically unrealistic limiting case of a rigid beam we have $k_1 \to \infty$ and $k_2 \to \infty$ and deflections and stresses in the plate will vanish. In this case we have a uniformly distributed shear force transmitted by the rigid beam to the flexible plate, but its intensity is of vanishingly small magnitude.

We thus conclude that the addition of a stiffening beam to the free edge of a cantilever plate strip can result in substantial reductions in plate stresses and deflections for the presently assumed loading condition. In effect, the stiffer the beam, the more uniformly the strain energy will be distributed in the plate.

Acknowledgements

Research reported herein was supported, in part, by the Air Force Office of Scientific Research under Grant No. AF-AFOSR-988-67. Computer facilities were generously made available by the Computing Center at State University of New York at Buffalo, which is partially supported by N.I.H. Grant FR-00126 and NSF Grant GP-7318.

VI. References

1. C. W. Mac Gregor, "Deflection of a Long Helical Gear Tooth". Mechanical Engineering, Vol. 57, No. 4, April 1935, p. 225–228.
2. D. L. Holl, "Cantilever Plate with Concentrated Edge Load". Trans. ASME, Journal of Applied Mechanics, Vol. 59, No. 1 Sep. 1937, p. A-8 to A-10.
3. T. J. Jaramillo, "Deflections and Moments due to a Concentrated Load on a Cantilever Plate of Infinite Length". Trans. ASME, Journal of Applied Mechanics, Vol. 72, No. 1 March 1950, p. A-67 to A-72.
4. L. I. Weingarten, "Effect of Shear Deflections on Edge Loaded Plate". Unpublished M.S. Thesis, State University of New York at Buffalo, Feb. 1966.
5. S. Timoshenko and S. Woinowsky-Krieger, "Theory of Plates and Shells". 2nd Ed., McGraw-Hill Book Co., Inc., New York, 1959.
6. K. Girkmann, „Flächentragwerke". 5th Ed., Springer-Verlag, Vienna, 1959.
7. I. N. Sneddon, "Fourier Transforms". McGraw-Hill Book Co., Inc., New York, 1951.
8. N. W. McLachlan, "Complex Variable Theory and Transform Calculus with Technical Applications". 2nd Ed., Macmillan Co., New York, 1953.
9. A. Ralston, "A First Course in Numerical Analysis". McGraw-Hill Book Co., Inc., New York, 1965.

Summary

A cantilever plate strip is reinforced by a beam bonded to its free edge. The opposite (parallel) edge is rigidly clamped. The beam is acted upon by a transverse concentrated load. Deflections and stresses are determined with particular reference to beam/plate stiffness ratios in bending and torsion.

Résumé

On renforce une plaque en console au moyen d'une poutre fixée à son bord libre. Le bord opposé (parallèle) est fixé de manière rigide. La poutre est solicitée par une charge transversale concentrée. Les flexions et les efforts sont déterminées d'une manière particulière par référence aux rapports de rigidité poutre-plaque pour la flexion et pour la torsion.

Zusammenfassung

Der Kragplattenstreifen ist durch einen Balken am freien Rand versteift, wobei der gegenüberliegende, parallele Rand fest eingespannt sein soll. Der Randträger wird durch eine Einzelkraft belastet. Durchbiegungen und Spannungen sind mit besonderer Berücksichtigung des Balken-Platten-Steifigkeitsverhältnisses in Biegung und Drillung bestimmt worden.